

## Supplemental material

# PUF-8 facilitates homologous chromosome pairing by promoting proteasome activity during meiotic entry in *C. elegans*

Ganga Anil Kumar and Kuppaswamy Subramaniam

## SUPPLEMENTARY METHODS

### Genetic mapping of *kp23*

The *kp23* mutation was mapped to chromosome V through standard 2-factor crosses using the reference strains EG1000 (*dpy-5(e61) I; rol-6(e187) II; lon-1(e1820) III*) and EG1020 (*bli-6(sc16) IV; dpy-11(e224) V; lon-2(e678) X*). Briefly, the mutant strain IT859 was mated with the reference strains and the recombination frequency between the *kp23* allele and the marker mutations of the reference strains were calculated by determining the fraction number of F2 clones that yielded progeny having both *kp23* and the marker phenotypes. The mating scheme is given as a flowchart in Fig. S1. The recombination frequencies were: 63% for *dpy-5* (n=19); 100% for *rol-6* (n=19); 47% for *lon-1* (n=19); 47% for *bli-6* (n=21); 9% for *dpy-11* (n=21) and 81% for *lon-2* (n=21).

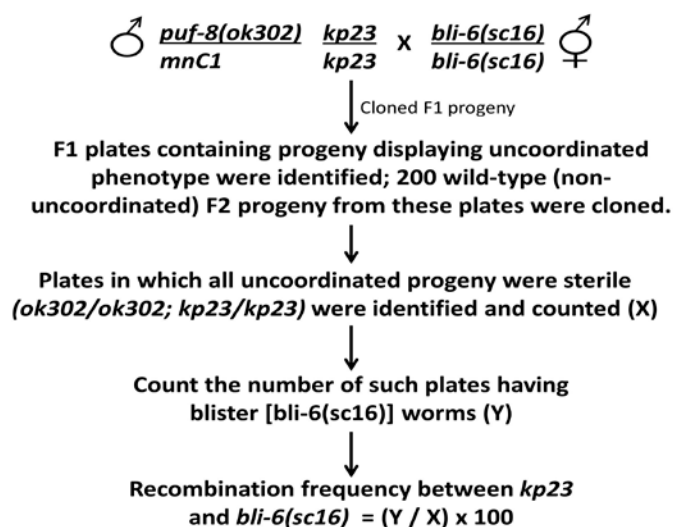


**Fig. S1. Flow chart describing the 2-factor genetic crosses.** The mating and recombination frequency calculation schemes with the *bli-6(sc16)* marker strain is shown here as an example. F2 worms were placed one hermaphrodite per plate (cloning) so that all F3 progeny present on a plate were from a single mother; thus, the genotype of the F2 worm could be inferred from the phenotypes of its progeny.

We performed whole genome sequencing and SNP analysis to further narrow down the position of *kp23* locus within chromosome V (Doitsidou et al., 2010). For this, we crossed IT859 worms with the polymorphic Hawaiian strain CB4586 and, by following the same strategy outlined in Fig. S1, selected the progeny of 27 cloned F2 worms that were homozygous for both *puf-8(ok302)* and *kp23*. These F2 progeny were pooled, and their genomic DNA was isolated and subjected to whole-genome sequencing. Genome sequencing and analysis were performed by GTAC, Washington University. As the DNA was isolated from worms homozygous for *kp23*, which is from N2 genetic background, CB4586-specific SNPs near the *kp23* locus is expected to be underrepresented in F2 *kp23* homozygotes. Indeed, CB4586-specific SNPs were particularly underrepresented between nucleotides 8,000,000 to 14,000,000 on chromosome V. Within this interval, there were nonsynonymous mutations affecting the coding sequences of *uig-1*, *pas-1*, and *coh-3*. RNAi-mediated depletion of UIG-1 and COH-3 in *puf-8(ok302)* worms did not show synthetic sterile phenotype; whereas depletion of PAS-1 by RNAi during larval stages caused *puf-8(ok302)*-dependent sterility, suggesting *kp23* might be an allele of *pas-1*. To further confirm the mapping results, we created the same G-to-A (substituting conserved glycine-20 with glutamic acid) change observed in *kp23* by CRISPR/Cas9 method; the resulting allele, named *kp72*, showed synthetic-sterile phenotype with *puf-8(ok302)* and the phenotype was indistinguishable from *puf-8(ok302); kp23* (Fig. S4).

### Mapping *kp78*

To map *kp78*, we sequenced the genomes of *puf-8(ok302) unc-4(e120)/mnC1 II; pas-1(kp72) V; kp78* and *puf-8(ok302) unc-4(e120)/mnC1 II; pas-1(kp72) V* worms. Comparison of both genome sequences revealed changes in 29 genes. Of these, only *rpn-1* was predicted to encode a

proteasome component; therefore, we created the same mutation isolated by the genetic screen in the wild-type genetic background using the CRISPR/Cas9 method (Fig. S11). The CRISPR allele, *kp85*, suppressed the *puf-8(ok302); pas-1(kp72)* phenotype, confirming that *kp78* is an allele of *rpn-1*.

### Construction of strains:

Strains IT1205 and IT1011: IT859 [*puf-8(ok302) unc-4/mnCI; pas-1(kp23)*] males were mated with OP227 L4 hermaphrodites. From the progeny of this cross, F1 males were selected and mated with uncoordinated hermaphrodites (*unc*) (*puf-8 unc-4/puf-8 unc-4*) of JH1500. Progeny from this mating were cloned and allowed to lay progeny. From plates having ‘unc’ (75% fertile and 25% sterile), paralyzed dumpy (*mnCI/mnCI*), GFP-positive progeny, 64 worms were cloned. The plates in which all ‘unc’ progeny were fertile and GFP-positive and all ‘unc’ progeny were sterile and GFP-positive were selected as IT1205 and IT1011, respectively.

Strains IT1013 and IT1119, IT1069 and IT1070, IT1017 and IT1016, IT1114 and IT1115 were generated as above by mating IT859 males with AV221, AV630, WH223 and CA1215 hermaphrodites, respectively.

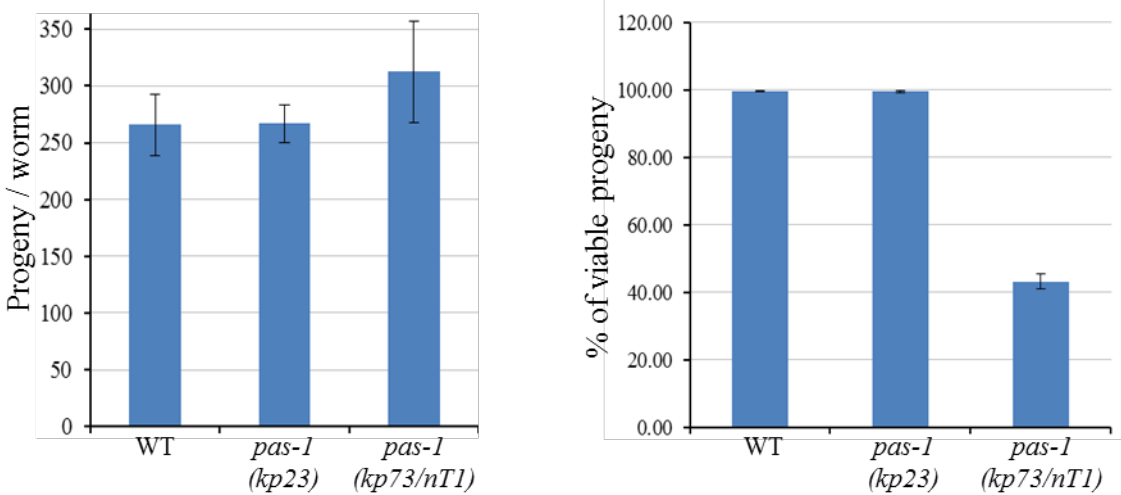
IT1188: IT859 males were mated with IT1187 L4 hermaphrodites and the resulting progeny were cloned at the L4-stage. Based on parental genotypes, half of these L4s were expected to yield some ‘unc’ progeny while the other half, some paralyzed dumpy progeny. From the plates having ‘unc’ progeny, 64 worms were cloned. A plate in which all ‘unc’ progeny were sterile and some progeny were GFP-positive was selected, and 20 worms from that plate were cloned.

Of these 20, the ones that did not yield any ‘unc’ progeny, but produced progeny that were all GFP-positive, was selected as IT1188.

IT1210: IT859 males were mated with IT1153 L4 hermaphrodites. Male progeny of this cross were mated with IT1188 L4 hermaphrodites. From the resulting progeny, 16 L4 larvae were cloned. After 48 hours, the cloned worms were lysed and subjected to single-worm PCR using the primers KS5295 and KS5296 to identify worms carrying *rpn-1(kp78)* allele. Sixty four progeny of a worm positive for *rpn-1(kp78)* were cloned. Of these 64, the ones that yielded progeny that were all positive for both GFP and the *kp78* allele were selected.

IT966: IT859 males were mated with IT396 hermaphrodites. F2 progeny of this cross were cloned and selected for a plate in which all ‘unc’ progeny were sterile and all progeny were GFP-positive.

All strains used in this study are listed in Table S1.

**Figure S2**

**Fig. S2. Effect of *pas-1* alleles on brood-size and embryonic viability.** The values are total number of embryos (left) and percentage of embryos that hatched (right) per worm of the indicated genotypes. In each case, the value represents the average from five worms. Note that the embryos homozygous for *nT1* are inviable; as a consequence, following Mendelian inheritance, 25% progeny of *pas-1(kp23)/nT1* are expected to be dead embryos due to *nT1*. Since about 60% progeny failed to hatch, all *kp73/73* homozygous and about 20% of *kp73/nT1* embryos were presumed to be dead due to the *kp73* mutation.

### Figure S3

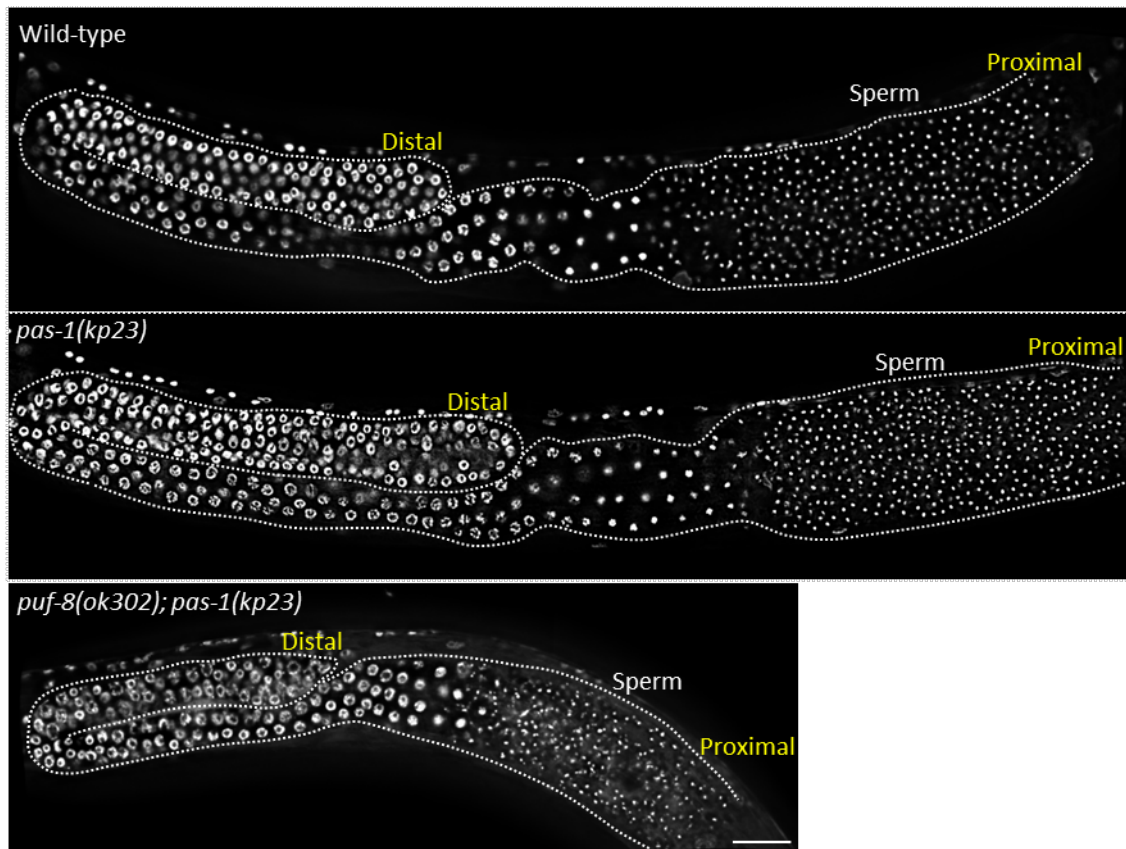


**Fig. S3. The *kp23* mutation does not affect spermatogenesis in males.** Adult males of the indicated genotypes were stained with DAPI. Germlines are outlined by dotted lines. Scale bar = 20 $\mu$ m.

## Figure S4

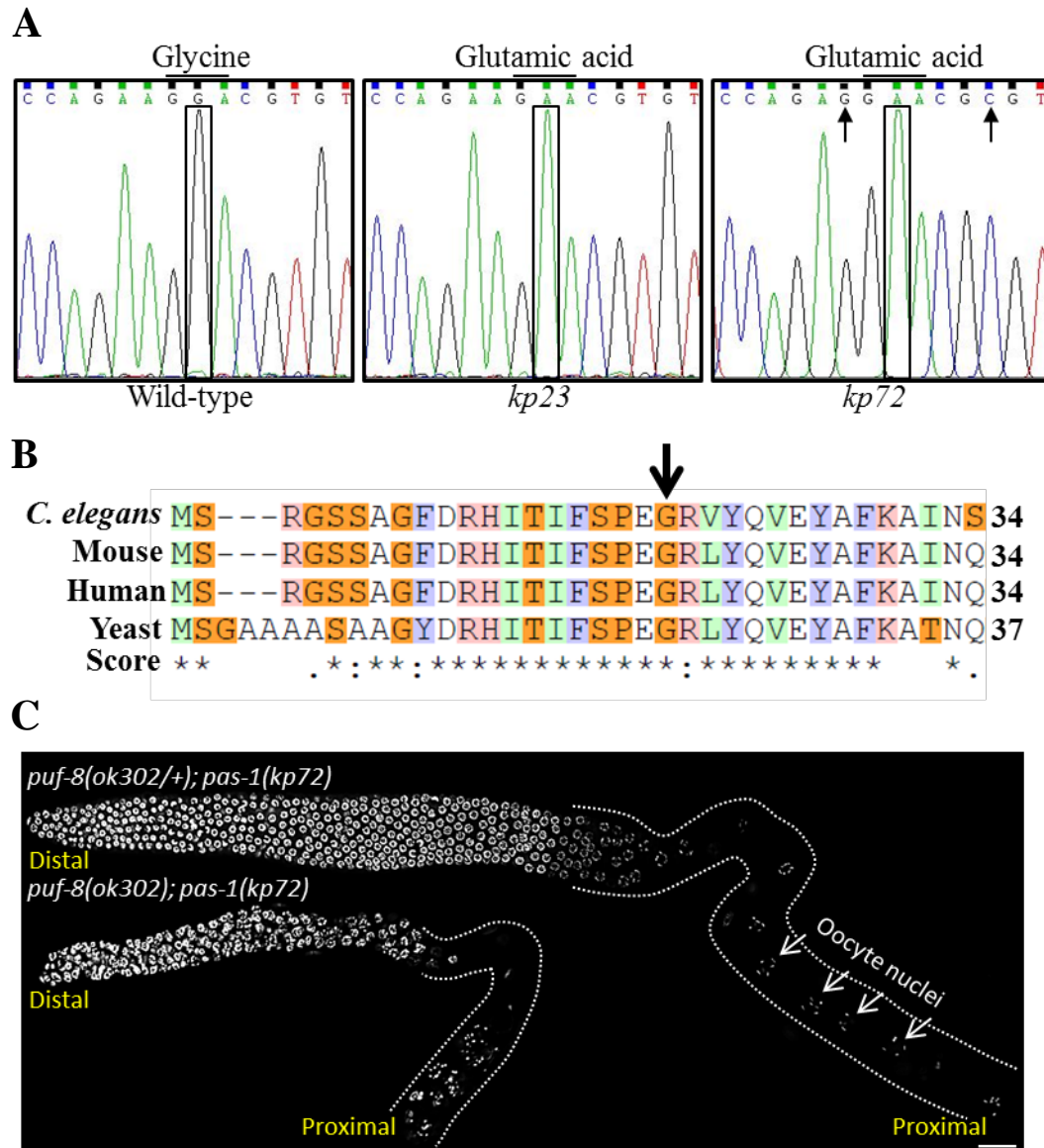


**Fig. S4. *kp23* is an allele of *pas-1*.** (A) Comparison of electropherograms of wild-type, *kp23*, *kp72* reveals a G-to-A change in the *pas-1* coding region of the mutant alleles. This single-base alteration replaces the conserved glycine residue at position 20 with glutamic acid. The arrows point to synonymous substitutions made to prevent re-cutting by Cas9. (B) Alignment of the N-terminal part of PAS-1 amino acid sequences. Arrow points to glycine-20. Asterisks, double-dots and single-dots mark perfectly conserved, highly conserved and semi-conserved residues, respectively. (C) Dissected gonads of the indicated genotypes stained with DAPI. Like the *puf-8(ok302); pas-1(kp23)* gonads, *puf-8(ok302); pas-1(kp72)* gonads do not have oocytes. Scale bar = 20µm.

## Figure S5

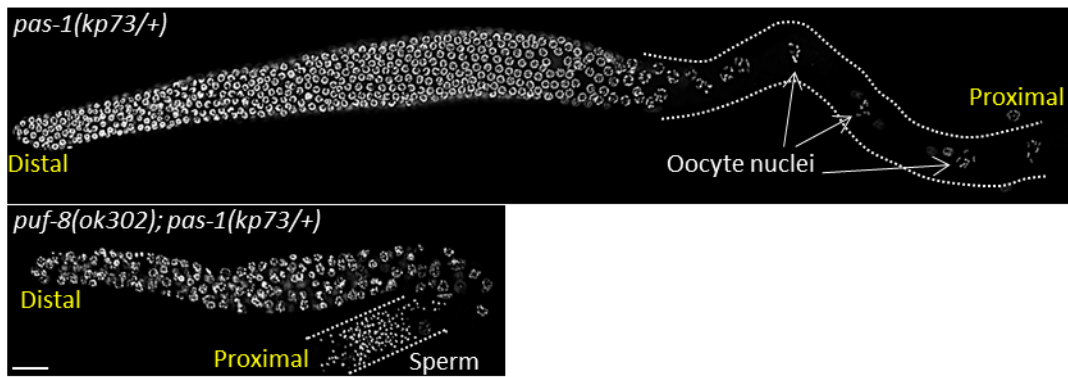
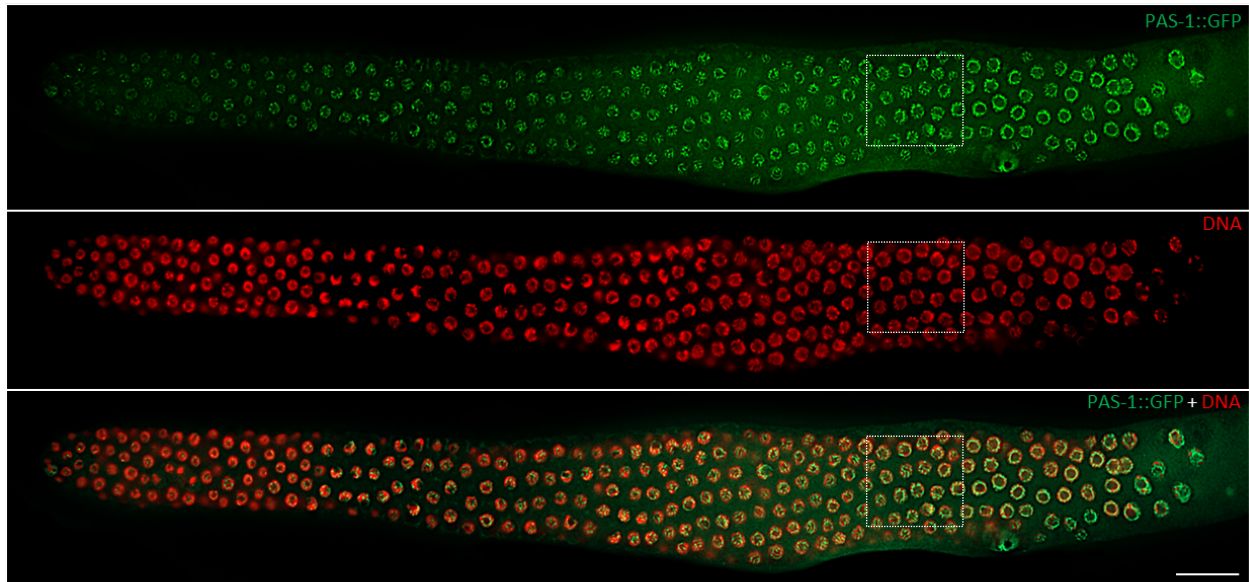


**Fig. S5.** The null allele, *kp73*, of *pas-1* exhibits haploinsufficient synthetic-sterility with *puf-8(ok302)*. Dissected gonads of the indicated genotypes stained with DAPI. Like the *puf-8(ok302); pas-1(kp23)* gonads (Fig. 1), *puf-8(ok302); pas-1(kp73/+)* gonads do not have oocytes. Scale bar = 20 $\mu$ m.

## Figure S6

A



B

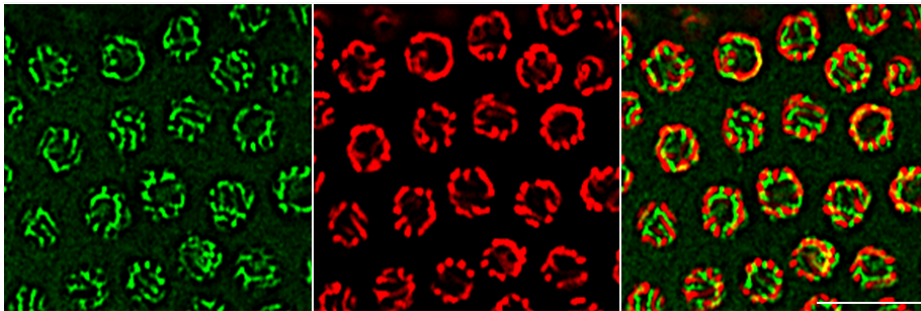


**Fig. S6. Distribution pattern of PAS-1 in the germline.** The presence of PAS-1 has been visualized by in-frame fusion of the GFP reporter at the C-terminus of PAS-1; coding sequences of GFP has been inserted at the endogenous *pas-1* locus using CRISPR/Cas9 method [strain IT1204]. **(A)** Distal arm of a dissected gonad stained with DAPI (red) is shown. Scale bar = 20 $\mu$ m. **(B)** Some pachytene nuclei [boxed area in **(A)**] are shown at higher magnification; PAS-1::GFP (green) localizes adjacent to chromatin (red). Scale bar = 10 $\mu$ m.

## Figure S7

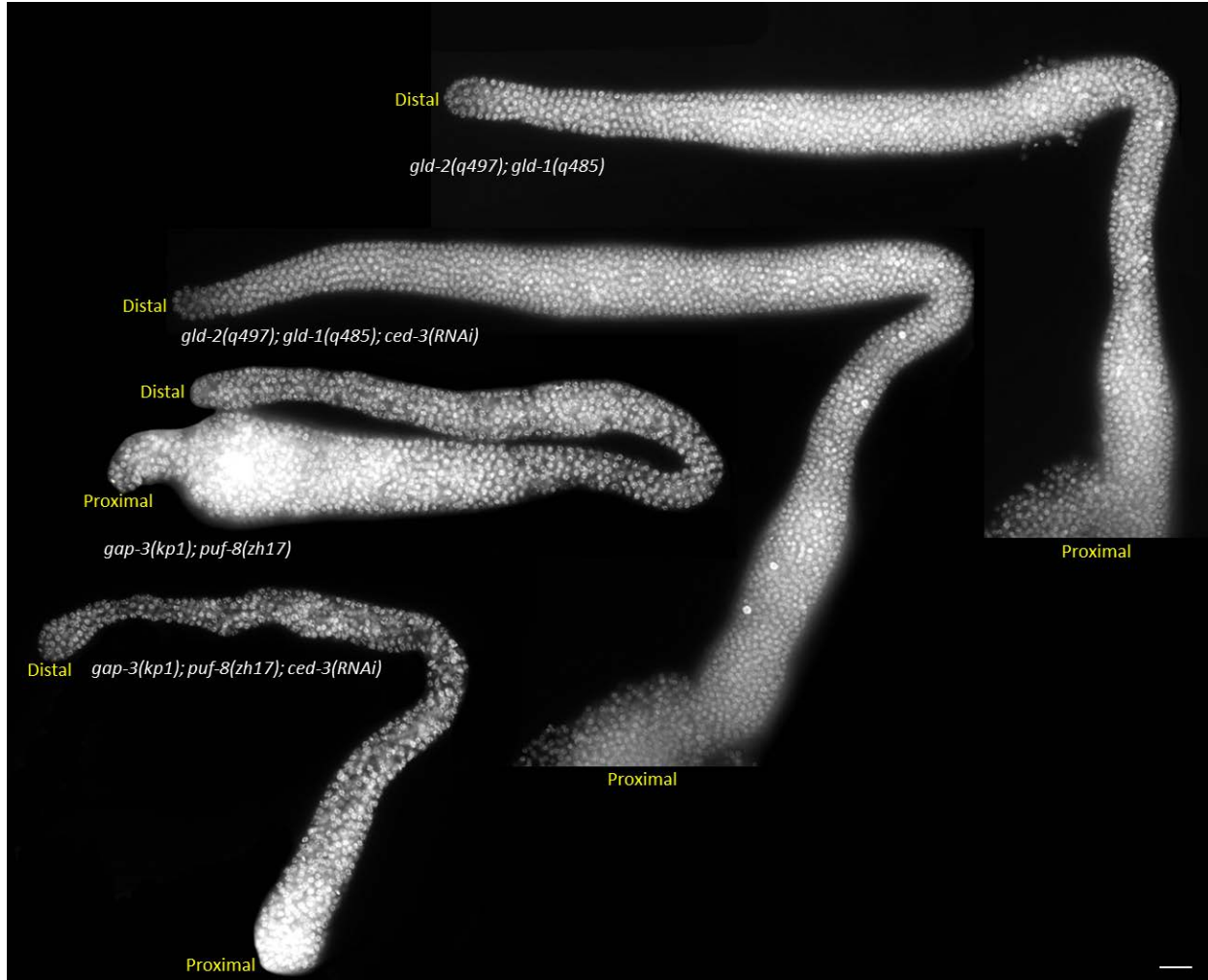


**Fig. S7. Effect of blocking apoptosis on mutants defective for meiotic entry.** Dissected gonads of the indicated genotypes stained with DAPI. In contrast to *puf-8(ok302); pas-1(kp23)* gonads (Fig. 2), *gld-2(q497) gld-1(q485)* and *gap-3(kp1); puf-8(zh17)* double mutants do not produce oocytes with univalent chromosomes upon inhibition of apoptosis by *ced-3(RNAi)*; instead, like the non-RNAi controls, they form germ cell tumor. For each genotype, 80 gonads were examined and all exhibited the same phenotype as shown here. Scale bar = 20 $\mu$ m.

## Figure S8

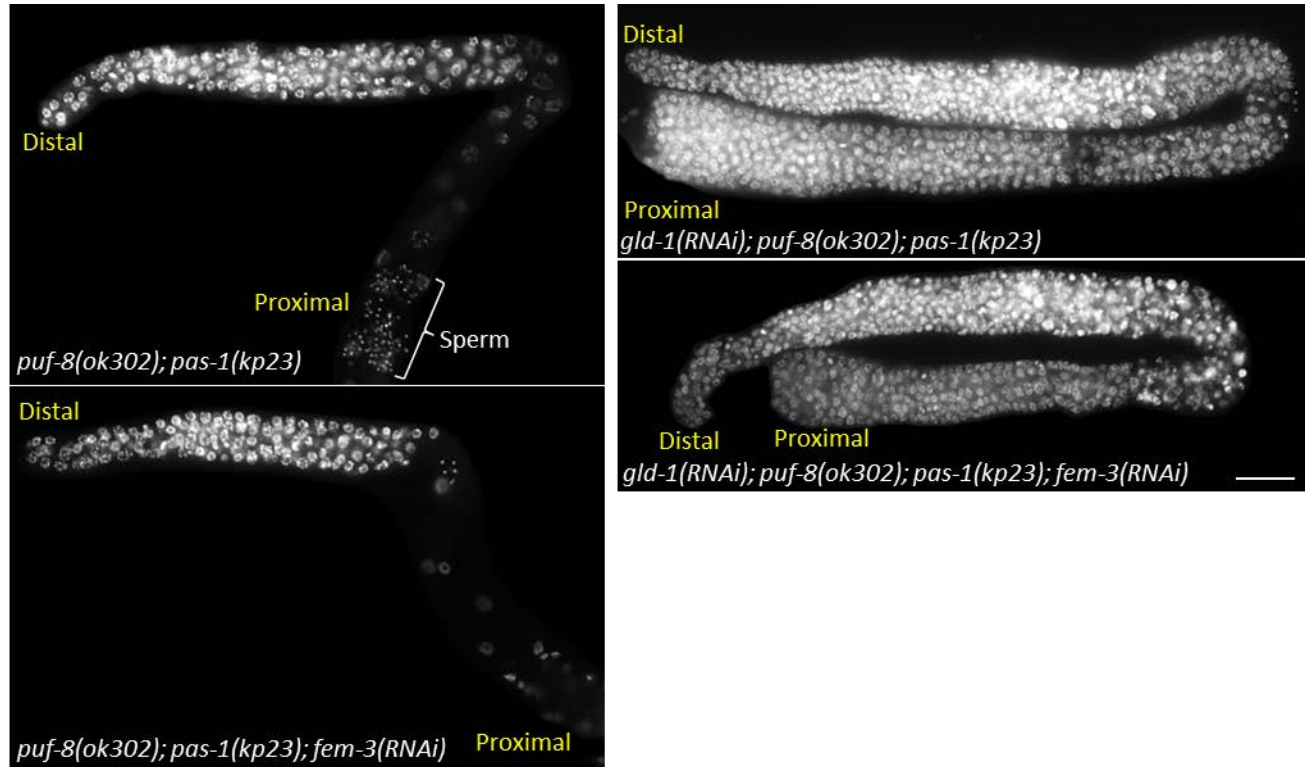


**Fig. S8. Meiotic entry-dependent tumor development is not affected by *puf-8(ok302); pas-1(kp23)*.** Dissected gonads of the indicated genotypes stained with DAPI. Female germ cells missing GLD-1 and male germ cells missing both GLD-1 and PUF-8 enter meiosis normally, but fail to progress through meiosis; instead, they dedifferentiate into germ cell tumors. Neither of these tumor formation is affected by *puf-8(ok302); pas-1(kp23)*, indicating that the *puf-8(ok302); pas-1(kp23)* germ cells enter meiosis normally. For each genotype, 80 gonads were examined and all exhibited the same phenotype as shown here. Scale bar = 20 $\mu$ m.

## Figure S9

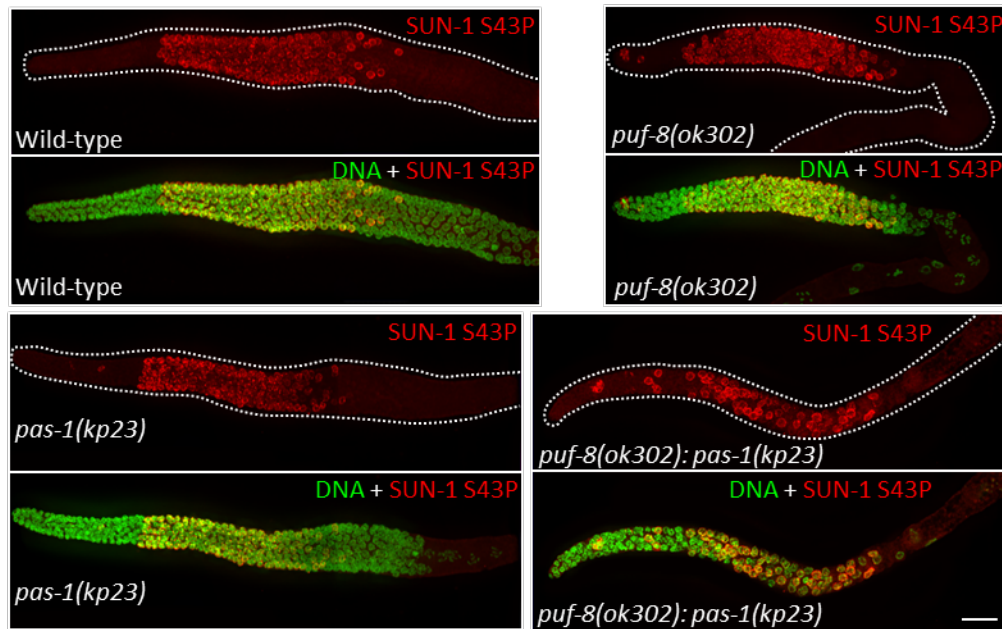


**Fig. S9. SUN-1 phosphorylation is not affected by *puf-8(ok302)*; *pas-1(kp23)*.** Dissected gonads of the indicated genotypes stained with antibodies specific for SUN-1 phosphorylated at serine-43 (SUN-1 S43P) and DAPI. In the wild-type, as expected, germ nuclei stain positively for SUN-1 S43P upon meiotic entry. Similar immunostaining pattern is observed in the other three genotypes as well, which supports that the *puf-8(ok302)*; *pas-1(kp23)* germ cells enter meiosis normally. Scale bar = 20 $\mu$ m.

**Figure S10**

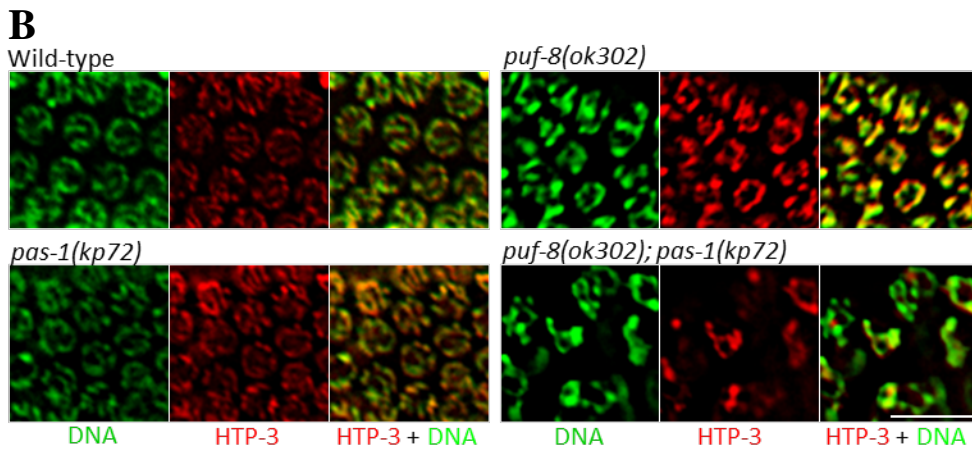
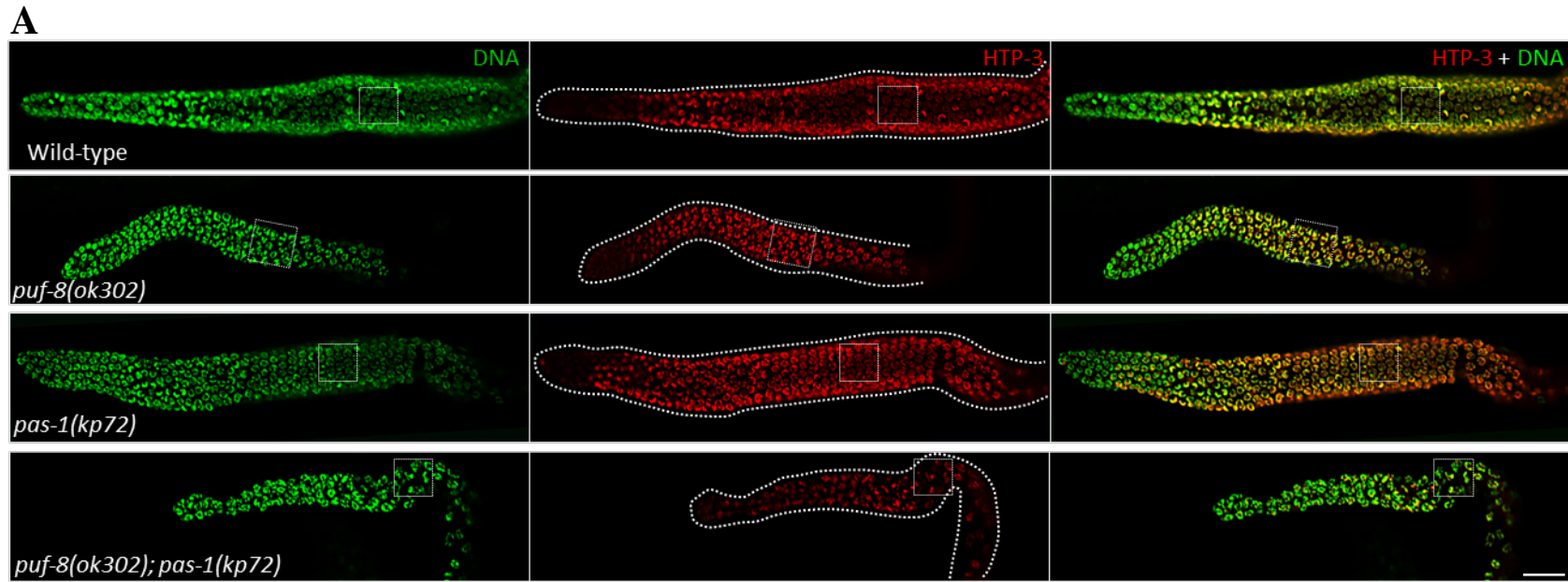


**Fig. S10. Distribution patterns of HTP-3 in wild-type, *puf-8(ok302)*, *pas-1(kp23)* and *puf-8(ok302); pas-1(kp23)* germlines. (A) Distal arm of dissected gonads of the indicated genotypes stained with anti-HTP-3 antibodies (red) and DAPI (green). Scale bar = 20µm. (B) Some pachytene nuclei [boxed area in (A)] at higher magnification. Scale bar = 10µm. While the distribution pattern of HTP-3 reveals aberrant chromosomal morphology in *puf-8(ok302); pas-1(kp23)* double mutant meiocytes, it does spread along the chromosomes in these cells.**

## Figure S11

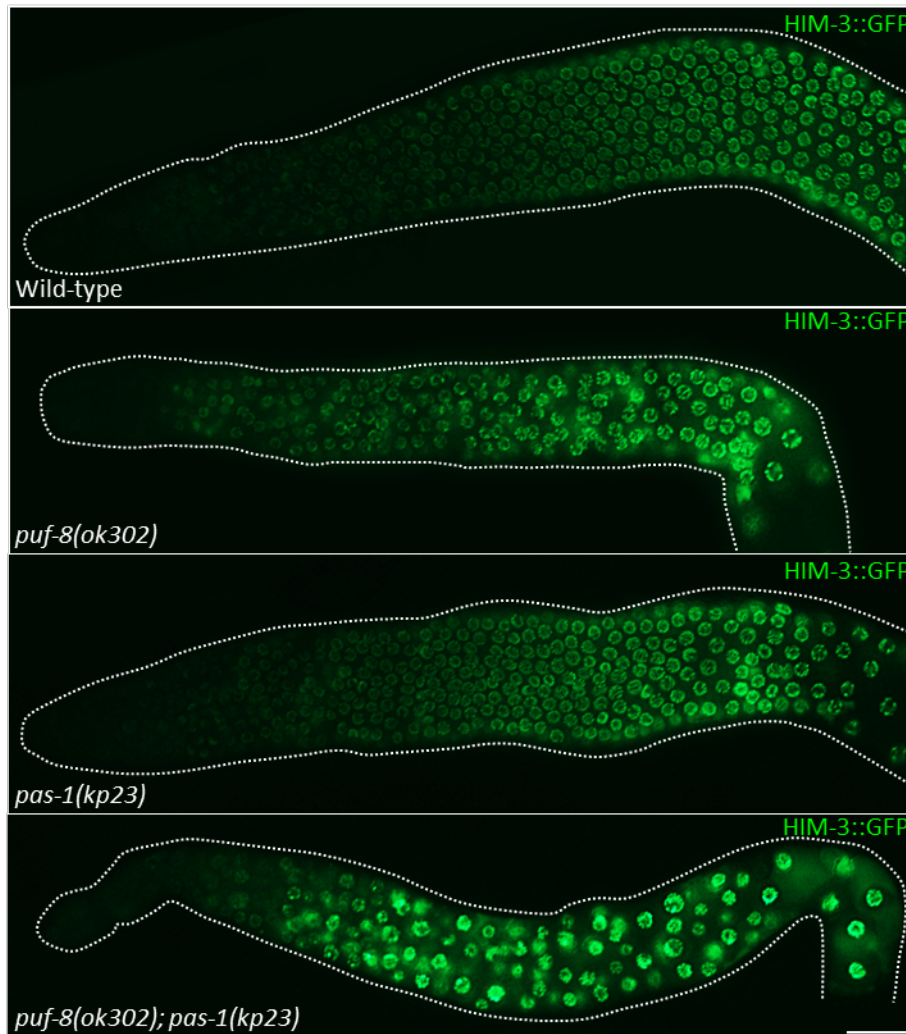


**Fig. S11. Distribution patterns of HIM-3 in wild-type, *puf-8(ok302)*, *pas-1(kp23)* and *puf-8(ok302); pas-1(kp23)* germlines.** Distal arm of dissected gonads of the indicated genotypes are shown [strains JH2120, IT396 and IT966]. The presence of HIM-3 has been visualized using a transgene that expresses HIM-3::GFP fusion protein (Merritt et al., 2008). Note that the onset of HIM-3::GFP expression is unaffected in the *puf-8(ok302); pas-1(kp23)* germline, although the fluorescence signal is somewhat brighter than the wild-type and reveals the aberrant chromatin morphology. Scale bar = 20 $\mu$ m.

## Figure S12

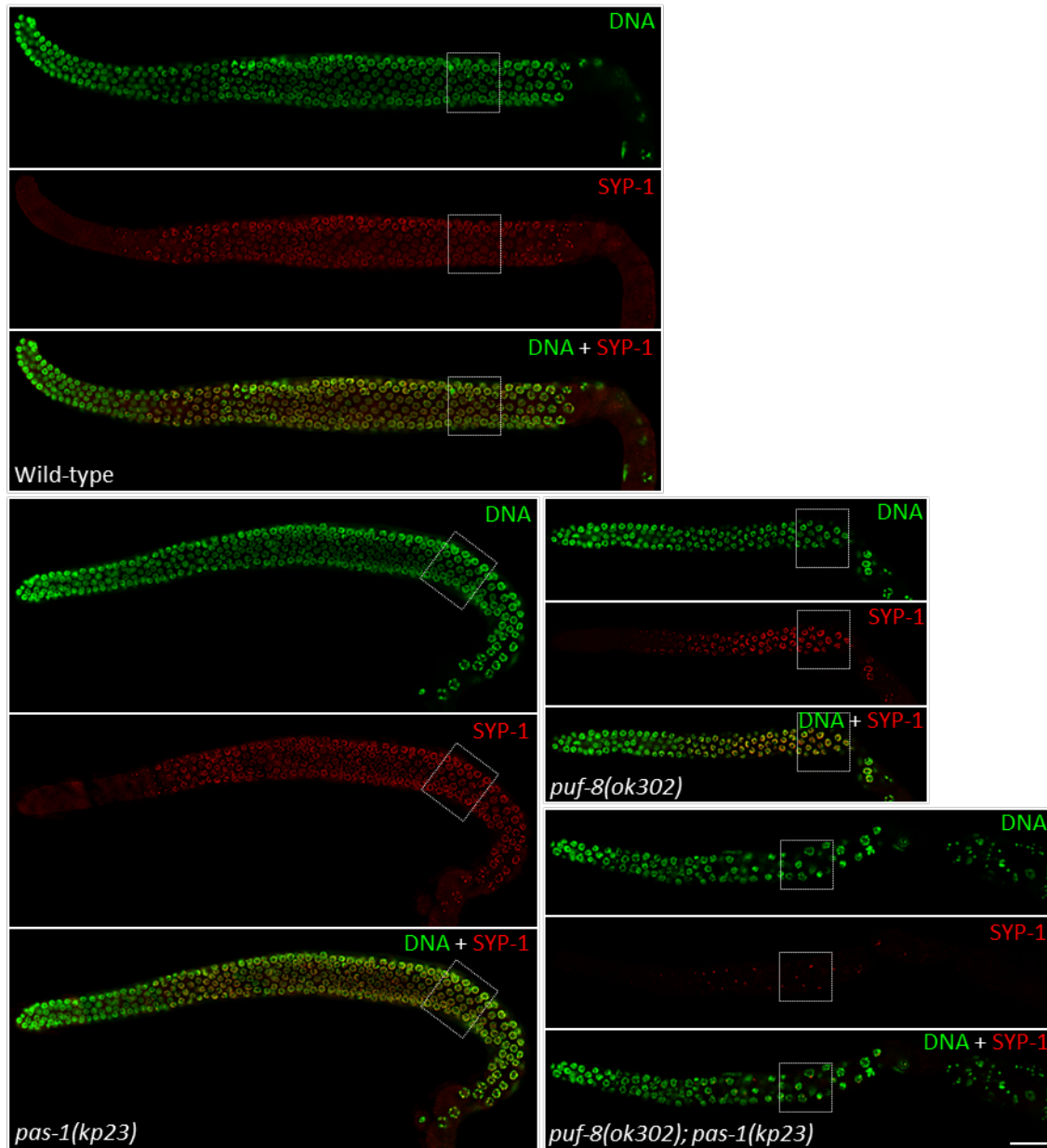


**Fig. S12. Distribution patterns of SYP-1 in wild-type, *pas-1(kp23)*, *puf-8(ok302)* and *puf-8(ok302); pas-1(kp23)* germlines.** Dissected gonads of the indicated genotypes stained with anti-SYP-1 antibodies (red) and DAPI (green) are shown. While SYP-1 spreads along meiotic chromatin in wild-type, *puf-8(ok302)* and *pas-1(kp23)* genotypes, it fails to spread and, instead, aggregates into specific foci in the *puf-8(ok302); pas-1(kp23)* double mutant. Boxed areas are shown at a higher magnification in Fig. 3. Scale bar = 20 $\mu$ m.

### Figure S13

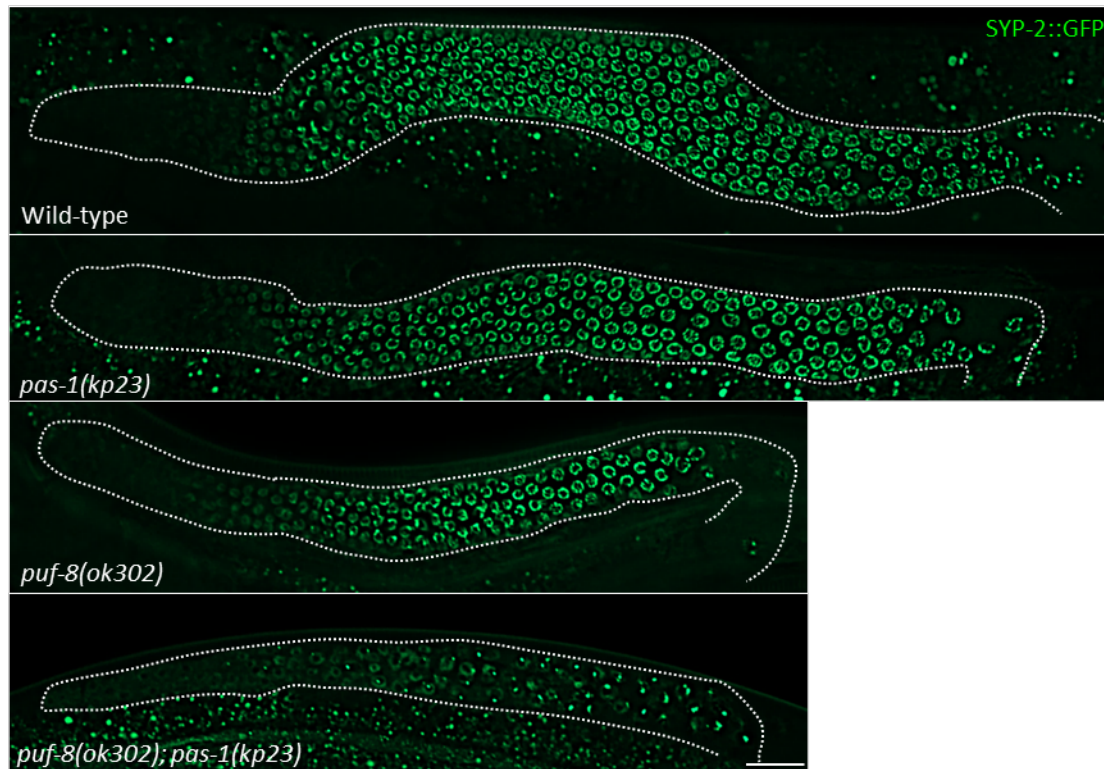


**Fig. S13. Distribution patterns of SYP-2 in wild-type, *pas-1(kp23)*, *puf-8(ok302)* and *puf-8(ok302); pas-1(kp23)* germlines.** Dissected gonads of the indicated genotypes expressing a transgene encoding SYP-2::GFP fusion protein are shown [strains OP227, IT1205 and IT1011]. Similar to SYP-1 aggregation (Fig. S9), SYP-2::GFP as well forms specific foci in the *puf-8(ok302); pas-1(kp23)* double mutant. Scale bar = 20 $\mu$ m.

Figure S14

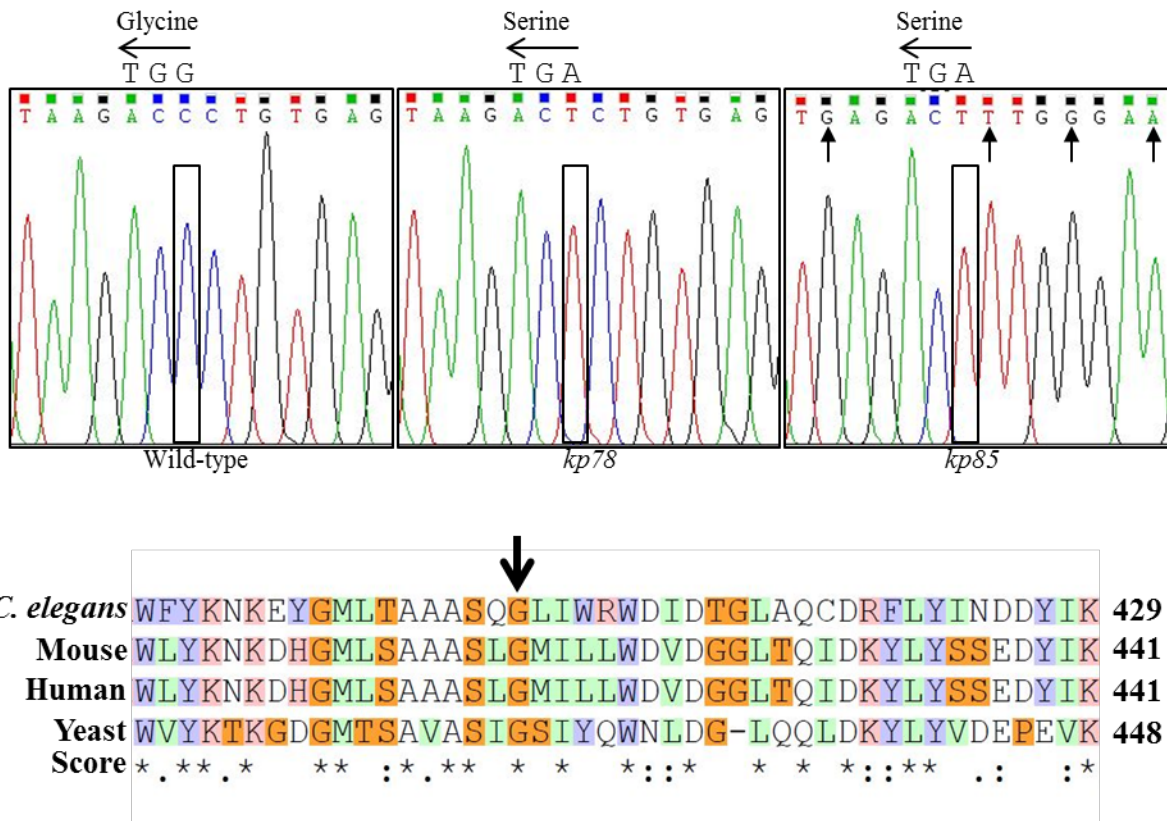


**Fig. S14. *kp78* is an allele of *rpn-1*.** (A) Comparison of electropherograms of wild-type, *kp78*, *kp85* reveals a G-to-A change in the *rpn-1* coding regions of the mutant alleles. This single-base alteration replaces the conserved glycine residue at position 403 with serine. Note that the electropherograms show the sequences of the non-coding strands. Arrows point to synonymous substitutions made to prevent re-cutting by Cas9. (B) Alignment of RPN-1 amino acid sequences around the region bearing the *kp78* mutation. Arrow points to glycine-403. Asterisks, double-dots and single-dots mark perfectly conserved, highly conserved and semi-conserved residues, respectively.

**Table S1. List of *C. elegans* strains used in this study**

Strain name	Genotype	Reference
JH1500	<i>puf-8(ok302) unc-4(e120)/mnC1 II</i>	(Subramaniam and Seydoux, 2003)
IT859	<i>puf-8(ok302) unc-4(e120)/mnC1 II; pas-1(kp23) V</i>	This study
IT1028	<i>puf-8(ok302) unc-4(e120)/mnC1 II; pas-1(kp72) V</i>	This study
IT1116	<i>puf-8(ok302) unc-4(e120)/mnC1 II; pas-1(kp73) V/nT1 [qIs51] (IV;V)</i>	This study
OP230	<i>unc-119(ed3) III; wgIs230[syp-1::TY1::EGFP::3xFLAG(92C12) + unc-119(+)]</i>	(Gerstein et al., 2010; Sarov et al., 2006)
OP227	<i>unc-119(ed3) III; wgIs227[syp-2::TY1::EGFP::3xFLAG(92C12) + unc-119(+)]</i>	(Gerstein et al., 2010; Sarov et al., 2006)
IT1205	<i>puf-8(ok302) unc-4(e120)/mnC1 II; wgIs227</i>	This study
IT1011	<i>puf-8(ok302) unc-4(e120)/mnC1 II; pas-1(kp23) V; wgIs227</i>	This study
IT1153	<i>puf-8(ok302) unc-4(e120)/mnC1 II; rpn-1(kp78) IV; pas-1(kp72) V</i>	This study
IT1161	<i>puf-8(ok302) unc-4(e120)/mnC1 II; rpn-1(kp85) IV; pas-1(kp72) V</i>	This study
AV221	<i>unc-119(ed3) meT8 (III); meIs4 meT8 (IV); meIs1</i>	(Bilgir et al., 2013)
IT1013	<i>puf-8(ok302) unc-4(e120)/mnC1 II; meIs4 meT8 (IV); meIs1</i>	This study
IT1119	<i>puf-8(ok302) unc-4(e120)/mnC1 II; meIs4 meT8 (IV); pas-1(kp23) V; meIs1</i>	This study
AV630	<i>meIs8 [pie-1p::GFP::cosa-1 + unc-119(+)] II</i>	(Yokoo et al., 2012)
IT1069	<i>puf-8(ok302) unc-4(e120)/mnC1 meIs8 II</i>	This study
IT1070	<i>puf-8(ok302) unc-4(e120)/mnC1 meIs8 II; pas-1(kp23) V</i>	This study
IT828	<i>unc-119(ed3) III; kpIs99 [pie-1p::GFP::H2B::drp-1 3' UTR; unc-119(+)]</i>	This study
IT1187	<i>unc-119(ed3) III; kpIs100 [pie-1p::Ub(G76V)::GFP::H2B::drp-1 3' UTR; unc-119(+)]</i>	This study
IT1188	<i>pas-1(kp23) V; kpIs100</i>	This study
IT1210	<i>rpn-1(kp78) IV; pas-1(kp23) V; kpIs100</i>	This study
IT1196	<i>htp-3(vc75) I; puf-8(ok302) unc-4(e120)/mnC1 II; pas-1(kp72) V</i>	This study
IT1204	<i>kpIs101 [pas-1::GFP] V</i>	This study
CA1215	<i>dhc-1(ie28 [dhc-1::degron::GFP] ) I; ieSi38 [sun-1p::TIR1::mRuby::sun-1 3'UTR + Cbr-unc-119(+)] IV</i>	(Zhang et al., 2015)
IT1114	<i>dhc-1(ie28[dhc-1::degron::GFP] ) I; puf-8(ok302) unc-4(e120) /mnC1 II; ieSi38 IV</i>	This study
IT1115	<i>dhc-1(ie28[dhc-1::degron::GFP] ) I; puf-8(ok302) unc-4(e120)/mnC1 II; ieSi38 IV; pas-1(kp23) V</i>	This study

WH223	<i>ojis9</i> [ <i>zyg-12(all)::GFP</i> + <i>unc-119(+)</i> ]	(Malone et al., 2003)
IT1017	<i>puf-8(ok302) unc-4(e120)/mnC1 II;ojis9</i>	This study
IT1016	<i>puf-8(ok302) unc-4(e120)/mnC1 II; pas-1(kp23) V;ojis9</i>	This study
JH2120	<i>axIs1534</i> [ <i>pie-1p::GFP::him-3 3'UTR</i> + <i>unc-119(+)</i> ]	(Merritt et al., 2008)
IT396	<i>puf-8(ok302) unc-4(e120)/mnC1 II; axIs1534</i>	Unpublished
IT966	<i>puf-8(ok302) unc-4(e120)/mnC1 II; pas-1(kp23) V; axIs1534</i>	This study
JK2879	<i>gld-2(q497) gld-1(q485)/hT2 [bli-4(e937) let-?(q782) qIs48] (I;III)</i>	(Kadyk and Kimble, 1998)
IT540	<i>gap-3(kp1) I; puf-8(zh17) unc-4(e120)/mnC1 [dpy-10(e128) unc-52(e444)] II</i>	(Vaid et al., 2013)

**Table S2. List of primers used in this study**

Name	Sequence	Description
KS2431	CTTTCGGACAACATCTCGTG	Forward for <i>pas-3(RNAi)</i>
KS2432	TCTCAGCAGTCTCAGCTTCC	Reverse for <i>pas-3(RNAi)</i>
KS4565	CAACAGTTACGTCGAACCGC	Forward for <i>uig-1(RNAi)</i>
KS4566	AAGATGGAGTTGCACTGCTG	Reverse for <i>uig-1(RNAi)</i>
KS4567	ATATGCCATGCGAGCTTCTC	Forward for <i>pas-1(RNAi)</i>
KS4568	CGGTTGGCGATTTGATTGAG	Reverse for <i>pas-1(RNAi)</i>
KS4569	CGTTGAAGACGATTTGGCTG	Forward for <i>coh-3(RNAi)</i>
KS4570	TCTTCTGCTCCTTCGTTCTC	Reverse for <i>coh-3(RNAi)</i>
KS4631	CGTAGGAAATGAACAAAAGAGC	Reverse to detect <i>pas-1(kp72)</i> and <i>pas-1(kp73)</i>
KS4739	CAAGACATCTCGCAATAGG	Reverse for cloning sgRNA template into pDD162; for generating <i>kp72</i> mutation
KS4740	CCTGATAAACACGTCCTTCGTTTTAGAGCTAGAAATAGCAAGT	Forward primer used along with KS4739
KS4761	CAGCGCCGGATTCGATCGTCATATTACCATCTTCTCTCCAGAGGAACGCGTCTACCAGGTTATAAAAATAATAGTTGAATGTTTATAAC	Repair template for <i>pas-1(kp72)</i>
KS4763	GAACCTCAATACGGCAAGATGAGAATGACTGGAAA CCGTACCGCATGCGGTGCCTATGGTAGCGGAGCTTACATGGCTTCAGACC	Repair template for <i>dpy-10(cn64)</i>
KS4764	TTTAAGGTGCGGTCACTCAA	Forward to detect <i>pas-1(kp72)</i> and <i>pas-1(kp73)</i>
KS4973	CAAAAAAACTAGCAATAAAGGAATAAAAACTGTACACCTTAAAGGCGC	Forward to amplify U6 promoter from pRB1017
KS4974	AAATTTACAAAAAGCACCGACTCGGTGCC	Reverse to amplify U6 promoter from pRB1017
KS4998	GATTCGATCGTCATATTACCATCTTCTCTCCAAGCTAGCAGAAGGACGTGTTTATCAGGTTATAAAAATAATAGTTGAATG	Repair template for <i>pas-1(kp73)</i>
KS5248	TCTTGTTACTGCAGCCGCCTCACA	Forward for sgRNA1 to make <i>rpn-1(kp78)</i>

KS5249	AAACTGTGAGGCGGCTGCAGTAAC	Reverse for sgRNA1 to make <i>rpn-1(kp78)</i>
KS5250	TCTTGCGCCTCACAGGGTCTTATC	Forward for sgRNA2 to make <i>rpn-1(kp78)</i>
KS5251	AAACGATAAGACCCTGTGAGGCGC	Reverse for sgRNA2 to make <i>rpn-1(kp78)</i>
KS5252	TCTTGCTCCAGATAAGACCCTGTG	Forward for sgRNA3 to make <i>rpn-1(kp78)</i>
KS5253	AAACCACAGGGTCTTATCTGGAGC	Reverse for sgRNA3 to make <i>rpn-1(kp78)</i>
KS5261	AAGAACAAGGAATATGGAATGCTTACTGCAGCCGC TTCCCAAAGTCTCATTGGAGATGGGATATCGATAC CGGCCTGGCACAATGC	Repair template for <i>rpn-1(kp78)</i>
KS5295	GCTTACTGCAGCCGCTTCCCAA	To detect <i>rpn-1(kp78)</i>
KS5296	GGATCAGGAAGTGAACGGAG	To detect <i>rpn-1(kp78)</i>
KS5428	TCTTGATACCGTCGACCTCGAGG	Forward for sgRNA1 to insert ub(G76V) into IT1828
KS5429	AAACCCTCGAGGTCGACGGTATCC	Reverse for sgRNA1 to insert ub(G76V) into IT1828
KS5430	TCTTGACCGTCGACCTCGAGGGG	Forward for sgRNA2 to insert ub(G76V) into IT1828
KS5431	AAACCCCCTCGAGGTCGACGGTC	Reverse for sgRNA2 to insert ub(G76V) into IT1828
KS5432	ATGGGATCCCCGGGCTGCAGGAATTCGATATCAA GCTTATCGATACCGTCGACCTCGAGATGCAGATCTT CGTGAAGAC	Forward for ub(G76V), template for CRSIPR/Cas9
KS5433	GACAACCTCCAGTGAAGTTCTTCTCTTTACTCAT TTTTTCTACCGGTACCGCCCCACCACCTCTGAG ACGGAGTA	Reverse for ub(G76V), template for CRSIPR-Cas9
KS5565	TCTTGATGAATATTTAATCTCGGT	Forward for sgRNA1 at the C-terminus of <i>pas-1</i>
KS5566	AAACACCGAGATTAATATTCATC	Reverse for sgRNA1 at the C-terminus of <i>pas-1</i>
KS5567	TCTTGGTCGATGAATATTTAATCT	Forward for sgRNA2 at the C-terminus of <i>pas-1</i>
KS5568	AAACAGATTAATATTCATCGACC	Reverse for sgRNA2 at the C-terminus of <i>pas-1</i>
KS5576	TCTGCAGGATCCAACCTACCAATCTGACGGC	Forward for 5' homology arm (repair template) of <i>pas-1</i>
KS5577	TCTGCAGGATCCATCTCGGTTGGCGATTTGATTGAG ATGATGTTTCGACCTGATCGTAGTTAGCTTAGTGAA TTTGGAGTTATCCTTGGTGAC	Reverse for 5' homology arm (repair template) of <i>pas-1</i>
KS5584	TTCGAAGCTTTTGGCGTCAT	Forward primer to detect <i>htp-3(vc75)</i>
KS5585	TGAATTCGAGGCATATGCG	Reverse primer to detect <i>htp-3(vc75)</i>

## Supplementary references

- Bilgir, C., Dombecki, C. R., Chen, P. F., Villeneuve, A. M. and Nabeshima, K.** (2013). Assembly of the Synaptonemal Complex Is a Highly Temperature-Sensitive Process That Is Supported by PGL-1 During *Caenorhabditis elegans* Meiosis. *G3 (Bethesda)* **3**, 585-595.
- Doitsidou, M., Poole, R. J., Sarin, S., Bigelow, H. and Hobert, O.** (2010). *C. elegans* mutant identification with a one-step whole-genome-sequencing and SNP mapping strategy. *PLoS One* **5**, e15435.
- Gerstein, M. B. Lu, Z. J. Van Nostrand, E. L. Cheng, C. Arshinoff, B. I. Liu, T. Yip, K. Y. Robilotto, R. Rechtsteiner, A. Ikegami, K. et al.** (2010). Integrative analysis of the *Caenorhabditis elegans* genome by the modENCODE project. *Science* **330**, 1775-87.
- Kadyk, L. C. and Kimble, J.** (1998). Genetic regulation of entry into meiosis in *Caenorhabditis elegans*. *Development* **125**, 1803-13.
- Malone, C. J., Misner, L., Le Bot, N., Tsai, M. C., Campbell, J. M., Ahringer, J. and White, J. G.** (2003). The *C. elegans* hook protein, ZYG-12, mediates the essential attachment between the centrosome and nucleus. *Cell* **115**, 825-36.
- Merritt, C., Rasoloson, D., Ko, D. and Seydoux, G.** (2008). 3' UTRs are the primary regulators of gene expression in the *C. elegans* germline. *Curr. Biol.* **18**, 1476-82.
- Sarov, M., Schneider, S., Pozniakovski, A., Roguev, A., Ernst, S., Zhang, Y., Hyman, A. A. and Stewart, A. F.** (2006). A recombineering pipeline for functional genomics applied to *Caenorhabditis elegans*. *Nat Methods* **3**, 839-44.
- Subramaniam, K. and Seydoux, G.** (2003). Dedifferentiation of primary spermatocytes into germ cell tumors in *C. elegans* lacking the pumilio-like protein PUF-8. *Curr. Biol.* **13**, 134-9.
- Vaid, S., Ariz, M., Chaturbedi, A., Kumar, G. A. and Subramaniam, K.** (2013). PUF-8 negatively regulates RAS/MAPK signalling to promote differentiation of *C. elegans* germ cells. *Development* **140**, 1645-54.
- Yokoo, R., Zawadzki, K. A., Nabeshima, K., Drake, M., Arur, S. and Villeneuve, A. M.** (2012). COSA-1 reveals robust homeostasis and separable licensing and reinforcement steps governing meiotic crossovers. *Cell* **149**, 75-87.
- Zhang, L., Ward, J. D., Cheng, Z. and Dernburg, A. F.** (2015). The auxin-inducible degradation (AID) system enables versatile conditional protein depletion in *C. elegans*. *Development* **142**, 4374-84.